Experimental study on ferritic stainless steel trapezoidal decks for composite slabs in construction stage

I. Arrayago*[a], E. Real[a], E. Mirambell[a], F. Marimon[b], M. Ferrer[b]

[a)] Department of Civil and Environmental Engineering, Universitat Politècnica de Catalunya, Jordi Girona 1-3, C1 Building (room 207), Barcelona 08034, Spain

[b)] Department of Strength of Materials and Structural Engineering, ETSEIB, Universitat Politècnica de Catalunya, Avinguda Diagonal 647, 08028 Barcelona, Spain

Corresponding author: Itsaso Arrayago, itsaso.arrayago@upc.edu, Tel: +34 934054156

ABSTRACT

The use of composite floor slabs is well established and provides an opportunity to promote the use of visually exposed composite slabs. Stainless steels, with the combination of good mechanical properties and excellent corrosion resistance, are key to this strategy, especially ferritic stainless steels, whose price is lower and more stable than that corresponding to the more widely used austenitic grades, due to their low nickel content whilst still maintaining good mechanical properties and aesthetic appeal. In addition, the emissivity of these grades contribute to lowering the heating and cooling requirements of buildings, reducing the costs associated to maintenance. Generally used as cold-formed members with high resistance-to-weight ratios, stainless steel decks are slender and highly sensitive to buckling phenomena and so the study of the structural performance of composite slabs using ferritic stainless steel decking is required due to the complex nonlinear behaviour of stainless steels, which is very different from that exhibited by carbon steel. Thus, this paper presents a comprehensive experimental programme on ferritic stainless steel trapezoidal decks for composite slabs under several structural configurations occurring during construction stage: simply supported decks under positive and negative bending moment, continuous decks and internal and end support tests. All the experimental results have been compared with the predicted ultimate loads in EN 1993-1-4, which remits to EN 1993-1-3

for carbon steel, and also with some previous tests on galvanized carbon steel decks, and it has been concluded that EN 1993-1-3 provisions are applicable to ferritic stainless steels.

KEYWORDS

ferritic stainless steel, stainless steel, steel decking, tests, trapezoidal deck

HIGHLIGHTS

- Experimental programme on ferritic stainless steel trapezoidal decks for composite slabs is presented.
- Simply supported, continuous deck, internal and end support tests are reported.
- The assessment of EN 1993-1-3 expressions for ferritic stainless steel decks is conducted.
- Tests results are compared to similar experiments on carbon steel decks.

1 INTRODUCTION

Decking profiles are commonly and widely used in steel-concrete composite construction, especially in floors and roofing. They are economic because the steel deck provides a formwork for concrete in relatively large spans supporting the self-weight of concrete as well as the construction loads without temporary propping between the beams, presenting several advantages in comparison to concrete structures. Decking profiles are usually obtained from cold-forming procedures, allowing economical manufacture of unusual sectional configurations and high strength-to-weight ratios, what also makes them susceptible to buckling phenomena due to their high slenderness. Other relevant advantages of steel decks are high strength and stiffness, light weight, simplicity for prefabrication and installation, allowing cost saving and making decks suitable for constructional purposes.

Trapezoidal sheets (or ribbed panels) have been used in building construction since 1780, so they represent one of the oldest types of cold-formed steel products. They do not only provide structural strength to carry loads, but they can also provide space for conduits or different services, water heating/cooling pipework and sound absorption material. Trapezoidal sheets have been often used as floor decks, wall panels, roofing, wall panels and bridge flooring, and their

fundamental behaviour has been systematically studied during the last decades [1-4], as well as their fire performance [5,6].

Stainless steels are relatively new metallic materials in construction, combining good mechanical properties and excellent corrosion resistance, which provide good ductility, formability and impact resistance, and make them ideal for structural purposes [7]. They also present better response at high temperatures than carbon steel and are durable, recyclable and aesthetic. With a chromium content of 10.5% and no more than 1.2% of carbon, many other elements can be also present in the composition in minor proportion for the different stainless steel families, such as molybdenum and nickel, providing resistance to special corrosive environments. Stainless steel is usually considered an expensive material, with considerable high requirements of initial investments, although when lifecycle costs are considered (including operating costs like maintenance and the residual value of the material), it can be considered a competitive material. However, stainless steels exhibit pronounced nonlinear stress-strain behaviour, even for low load levels, which make them different from carbon steels but which shows similarities with other construction materials such as cold-worked steel and aluminium. In addition, they usually present considerable strain hardening, showing an important strength reserve.

Ferritic stainless steels differ from the other families in the absence of nickel, an alloying element whose price has reached unprecedented levels and suffers continuous fluctuations. Their lower and more stable price make ferritic stainless steels especially attractive over the most common austenitic grades, keeping adequate mechanical properties and corrosion resistance [8], while they distort less when heated during welding. The lower thermal expansion coefficient and emissivity of ferritic stainless steels allow the mobilization of their thermal capacity in visually exposed composite floor slabs as part of an energy saving strategy, reducing the heating and cooling requirements in buildings.

All those mechanical and physical properties make ferritic stainless steels appropriate for their structural application, specially when high durability and aesthetic superficial finish are required.

In addition, they do not require any protection layers as painting and are easier to recycle than galvanized steels.

The use of composite floor slabs is well established and the design approach is presented in several codes such as Eurocode 4 EN 1994-1-1 [9]. However, ferritic stainless steel decking has not been used until the last years. An example of a use of stainless steel deck for roofing can be seen in Figure 1. The part of Eurocode corresponding to structural stainless steel is EN 1993-1-4 [10], although referring to the trapezoidal decking, a lack of a specific guideline for stainless steels is observed. Hence, EN 1993-1-4 [10] remits to EN 1993-1-3 [11], which represent the supplementary rules for cold-formed members and sheeting in carbon steel. Stainless steels show a strongly nonlinear behaviour even for low stress values, differing from carbon steel with a bilinear behaviour with a clearly defined yielding strength. Therefore, the applicability of the expressions codified in [11] needs to be assessed for stainless steels in general and for the ferritic ones in particular, in order to determine whether some new expressions need to be included in EN 1993-1-4 [10] or the same provided in EN 1993-1-3 [11] can be used. In addition, these steel sheets usually include some embossments which improve the connection between the steel and the concrete (see Figure 2), thus making the formulation of reliable models more difficult for analytical or numerical analysis. For this reason, conducting comprehensive experimental studies of steel sheets following adequate test arrangements (such as those provided in EN 1993-1-3, Annex A [11]) is important and valuable.

Figure 1. Profiled stainless steel decking [12].

The *Structural Applications in Ferritic Stainless Steel (SAFSS)* European Project, part of the Research Fund for Coal and Steel research program, was executed between July 2010 and December 2013 to provide the necessary information for the development of new design guides for ferritic stainless steels. The research work presented in this paper was part of this Research Project and intended to cover part of this lack of information and contribute to the developement of appropriate design guidelines for ferritic stainless steels by studying the structural behaviour of some stainless steel decking structures. This paper presents the experimental programme on

ferritic stainless steel decks in construction stage, comprising simply supported and continuous deck tests, as well as internal support and end support tests. All experimental results have been compared with the predicted ultimate loads according to EN 1993-1-4 [10] and EN 1993-1-3 [11], and also with some previous tests conducted at the Universität Karlsruhe [13] on galvanized carbon steel decks with identical cross-section to that studied in this paper.

2 TESTS ON FERRITIC STAINLESS STEEL DECKS

2.1 DECK AND MATERIAL DESCRIPTION

The cold-formed trapezoidal ferritic stainless steel deck considered in this experimental study can be seen in Figure 2, and it is usually conceived for moderate loading and medium size spans. The studied profile is 58 mm high and presents a total width of 1035 mm, involving five corrugated waves. The upper part of the waves is reinforced with two stiffeners, while the lower wave shows a single stiffener. A detailed geometrical definition of a representative wave is shown in Figure 3. The thickness of the studied stainless steel decks was measured and the average value was equivalent to the nominal thickness, 0.8 mm. Webs are inclined with a 72º angle and present embossments to guarantee a good connection between the deck and the concrete. These embossments show an inclination of 60º and different direction in both webs for each wave. The depth of embossments was measured on several waves of this profile and provided an average value of 2.78 mm.

Figure 2. Cofraplus 60 geometry [15].

Figure 3. Detailed geometry of a representative wave of the studied deck.

Table 1 summarizes different parameters of the mechanical properties of the profile for positive and negative bending, since the cross-section is not symmetrical about the horizontal axis, according to EN 1993-1-3 [11] calculations. In this table A is the gross-section area, I_0 and I_{eff} correspond to the second moment of area corresponding to the gross and effective sections and W_{el} and W_{eff} refer to the elastic and effective section moduli. It is important to mention that the effective section moduli reported in Table 1 have been obtained following the traditional Effective

Width Method prescriptions from EN 1993-1-3 [11] but with the specific rules given for stainless steels in EN 1993-1-4 [10], in which the existence of the embossments has not been considered. Some previous research works [16,17] have demonstrated that embossments decrease the flexural response of the sheets, but they increase the stiffening respect to web shear buckling and the local failure in the supports, although there is no consolidated theoretical model to consider the influence of these embossments.

Table 1. Mechanical properties for the studied deck from EN 1993-1-4 [10] and EN 1993-1-3 [11] calculations.

The stainless steel grade chosen for the experimental programme is the most usual EN 1.4003 ferritic grade. Table 2 shows the key material parameters defining the stress-strain behaviour of this material, obtained from several tensile coupon tests cut from the cold-formed section. E is the Young's modulus, $\sigma_{0.2}$ is the proof stress corresponding to a 0.2% plastic strain, conventionally considered as the yield stress, σ_u and ε_u are the ultimate strength and strain, respectively, and *n* and *m* are the strain hardening exponents.

Table 2. Key material properties of the studied stainless steel deck.

Since results corresponding to the tests conducted on galvanized steel and reported in [13] are not publicly available, the most relevant experimental results and parameters are summarized in Table 3. The nominal thickness of the galvanized steel decks is 0.75 mm, while the core thickness has been estimated from the measured average thickness by adopting the usual zinc coating thickness given in EN 1993-1-3 [11], t_{zinc}= 0.04 mm.

Table 3. Summary of key parameter and results from the experimental programme on galvanized steel decks [13].

2.2 SIMPLY SUPPORTED DECK TESTS

The bending moment resistance of the studied deck was determined by conducting a total of six simply supported deck tests, three of which were tested under a positive bending moment configuration, while the remaining three tests corresponded to a negative bending configuration. The test configuration was defined according to EN 1993-1-3, Annex A [11] prescriptions, using

the same set up for both positive and negative bending moment tests. Decks had a total length of 3100 mm, with a span length of 3000 mm and were subjected to four transversal loads. Loaded sections were those located at a distance of 375 mm and 1125 mm from each of the support sections, arranged to approximate uniformly distributed loading and introduced at the lower flanges of the cross section (see Figure 4a). Decks were simply supported, allowing for free rotation and longitudinal displacement at one of the supports, while only the rotation was set free for the other. Spreading of waves was prevented by using transverse ties under the loading sections, and the support sections were stiffened by using rectangular hollow sections and timber pieces. The weight of this upper loading structure was 900 N and has been added to the load values measured from the load cell. Given that the self-weight of the sheet represents less than 1.8% of the reached collapse load of simply supported tests (and even less for the rest of experimental configurations), it has been neglected in the results presented in this paper. The vertical deflections of the decks were measured at the midspan sections by two linear displacement transducers. Figure 4b shows one of the collapsed decks after the positive bending test.

Figure 4. General views of simply supported deck a) test configuration and b) after collapse.

The load-deflection curves for the six simply supported deck tests are presented in Figure 5, where M+ and M- correspond to positive and negative bending tests, respectively. All decks failed by local buckling at the midspan section (see Figure 4b), with a considerable more ductile response for the positive bending configuration because the yielding occurs first at the tension edge and plastic reserves in this zone can be mobilized. Table 4 reports the experimental results for the conducted simply supported ferritic stainless steel deck tests, where ultimate loads F_u and the corresponding ultimate moment M_u are reported for positive and negative bending configurations, together with the average midspan deflections d_u corresponding to the maximum loads. Characteristic values calculated according to [11] are also presented in this table. For this, EN 1993-1-3, A6.3 [11] states that the characteristic value of a set of experimental results should be calculated by multiplying the mean value by a factor η_k, which can adopt values between 0.8 and

0.9 for failure modes involving local buckling. Hence, a value of η_k=0.85 has been adopted in the calculation of the characteristic values throughout this paper.

As mentioned before, the resistance of trapezoidal cross-section carbon steel decks with the same cross-section and similar tests configurations was investigated at the Karlsruhe University and reported in [13]. The investigated decks corresponded to a S350GD+Z galvanized carbon steel with a measured average yield strength f_y = 411 MPa, higher than the strength of the ferritic stainless steel considered in this paper, with $\sigma_{0.2} = f_y$ = 326 MPa (see Table 2). The tested cross-sections were also equivalent, although ferritic stainless steel decks were 0.8 mm thick whereas carbon steel decks showed an average core thickness of 0.74 mm. These differences have been considered in the comparison of experimental results for simply supported decks, as well as for the following sections, by adopting the approach given in EN 1993-1-3, A6.2 [11]. According to these clauses, experimental results corresponding to galvanized carbon steel have been adjusted by the factor $\mu_R=(f_{y,carbon}/f_{y,stainless})\cdot(t_{carbon}/t_{stainless})^2$=1.08. For comparison purposes, weights of loading upper structures equivalent to those reported in this paper have been considered for the experimental programme conducted by [13], as no relevant data is provided in the report.

In addition, the test configuration arranged in [13] for positive bending tests was identical to that considered in this paper, although the cross-section used in [13] for the negative bending tests was narrower than the one analysed in this study, involving four waves instead of the five waves of the present cross-section shown in Figure 2. Therefore, it is necessary to transform the ultimate loads reported in [13] for negative bending tests in order to make them comparable $P_{comp} = P_{test}\,5/4$. All these experimental results corresponding to simply supported decks for positive and negative bending moment are shown in Table 4, where it can be appreciated that failure bending moments are similar, although ultimate loads corresponding to the tests presented in this paper are slightly higher, probably due to strain hardening effects.

Figure 5. Load-displacement curves for simply supported ferritic stainless steel deck tests.

Table 4. Experimental results for simply supported ferritic stainless steel deck tests (width=1035mm).

2.3 CONTINUOUS DECK TESTS

Three continuous deck tests over two 3000 mm length spans were also conducted in order to determine the resistance of the deck subjected to a combination of moment and concentrated force at internal supports, so as to compare results with the ultimate bending moments obtained from single span tests. The test set up was also determined according to EN 1993-1-3, Annex A [11] specifications, where the uniformly distributed load was introduced through four transverse line loads using one 4 m long HEB 200 beam, two 2 m long HEB 120 beams and four 1.1 m long 80x80 square hollow section (SHS) beams (see Figure 6 and Figures 7a, 7b). It should be noted that among the alternatives given in EN 1993-1-3, Annex A [11] for simulating uniform loading conditions, the distribution provided by the option considered in this experimental programme is slightly less uniform. The weight of the loading upper structure (1800 N) has been added to the load values obtained from the load cell but the self-weight of the sheet was neglected. Hinged supports were placed at internal supports (Figure 7c) and roller supports at the ends of the decks (Figure 7d), all support sections being stiffened as for simply supported tests. Spreading of waves was also prevented by using transverse ties under the loading sections. In addition, middle support reactions were measured using two load cells to study bending moment redistribution and vertical deflections at midspan sections were measured by four linear variable differential transducers.

Figure 6. Test set-up for two span bending or continuous deck tests.

Figure 7. General views of continuous deck a) test configuration, and b) after collapse, c) hinged internal support and d) roller external support.

The load-displacement curves for all three tests are shown in Figure 8, where a change in the stiffness can be observed at the point at which the internal support fails (around 37 kN), but specimens do not collapse until higher loads are reached (around 40 kN). The initial failure of the decks occurred at the middle support section for all the conducted tests due to buckling of the compressed area of the cross-section (see Figure 7b). Test results for continuous decks are summarized in Table 5, where failure loads F_u and middle support collapse loads $F_{supp,coll}$ are

reported, as well as average midspan deflections at failure d_u and the characteristic values calculated from EN 1993-1-3, A6.3 [11].

Figure 8. Load-displacement curves for continuous deck tests.

Table 5. Experimental results for continuous ferritic stainless steel deck tests (width=1035mm).

2.4 INTERNAL AND END SUPPORT TESTS

Finally, the behaviour of the deck under local transverse forces was investigated through a series of internal and end support tests. In the former, the behaviour under the combination of bending moment and local transverse force is analysed, while the latter investigates the resistance of edge supports.

2.4.1 Internal support tests

The failure of profiled decks is usually governed by a combination of bending moment and support reaction at internal supports during floor construction, limiting the spanning capacities. Therefore, the behaviour of such regions of the continuous decks needs to be carefully tested and analysed by conducting three-point bending tests that simulate an inverted deck element at the middle support. The bending moment-transverse load interaction diagram was characterized by conducting nine internal support tests, three for each of the considered span lengths *s*, 1200 mm, 705 mm and 430 mm, although the total length of all specimens was 1300 mm in all cases.

The 1200 mm span length corresponds to the distance between points with zero bending moment estimated from the continuous decking tests described in the previous section from the measurement of the different support reactions. This value is similar to that proposed in EN 1993-1-3, Annex A [11] and the literature, where a span length of $s = 0.4 \cdot L = 0.4 \cdot 3000$ mm = 1200 mm is suggested. Span lengths of 705 mm and 430 mm were also included in the experimental programme in order to correctly characterize the bending moment-concentrated load interaction, according to [13].

All tests were conducted according to EN 1993-1-3, Annex A [11]. Decks were simply supported and subjected to a concentrated load at the midspan section, which was uniformly introduced by

a transverse IPN120 steel beam (the weight of the loading upper structure is 170 N) and directly applied on the specimen to simulate the internal support effect of a continuous beam, as shown Figure 9a. However, and in order to prevent end support failure, both support sections were stiffened by short SHS beams (see Figure 9b) and spreading of the waves was prevented by using transverse ties under the loading section. The vertical displacement of six points was measured for each of the conducted tests by means of linear variable differential transducers located at the midspan sections and at a distance of 100 mm from each support section, on both sides of the decks.

Figure 9. General views of internal support test a) configuration, b) view of the general collapse of the deck, c) lateral view of the general collapse and d) failure of the loading section.

Figure 10 shows the load-average deflection curves corresponding to the midspan section for the nine internal support tests conducted on ferritic stainless steel decks. Failure occurred at the loaded sections, due to the web crippling of the webs and the local buckling of the compressed areas, as shown in Figures 9c and 9d. Experimental results are reported in Table 6, where ultimate loads F_u and average midspan deflections d_u are provided, as well as the corresponding bending moment M_u, along with the characteristic values. Table 6 also summarizes the results from the internal support tests conducted at Karlsruhe University [13], where s = 430 mm and s = 705mm spans were investigated. The consideration of the differences in the yield strength and thickness has been considered following the approach described in Section 2.3. The similarity of the reported test results for the repeated span lengths is remarkable, although the ultimate load values are quite higher for the ferritic stainless steel deck tests, in line with those reported for simply supported decks in section 2.2.

Table 6. Experimental results for internal support tests on ferritic stainless steel decks (width=1035mm).

Figure 10. Load-displacement curves for internal support tests.

2.4.2 End support tests

Finally, four web crushing or end support tests were conducted in order to simulate the outer supports of the continuous deck tests and evaluate the resistance of the deck to concentrated transverse loads in absence of bending moment. Tests were also carried out following prescriptions given in EN 1993-1-3, Annex A [11] specifications. The influence of the distance from the internal edge of the end support to the end of the deck *u* was investigated, as suggested in [11], by testing two of the decks with a distance of *u*=40 mm, and two more with *u*=60 mm. Since only one part of the deck was tested in specimens with *u*=40 mm, the opposite side remained undeformed and so new tests with *u*=60 mm were conducted in these undeformed sides. Figures 11a and 11b present the general views of the conducted end support test configurations for *u*=40 mm and *u*=60 mm, respectively. Alternatively, Figures 11c and 11d show the detailed view of the collapse of one of the decks and the failure of the end support section.

Figure 11. Views of a) end support test configuration for *u*=40 mm, b) general view of failed deck for *u*=40 mm, c) detailed view of the collapse of the deck and d) failure of the end support section.

The decks were tested under simply supported conditions, a rib was used to guarantee that the load at the rolling supports was applied as a line-load and the hinge supports were stiffened by using SHS short elements. The load was applied in a bearing length s_s of 300 mm, as proposed in [11], by welding three 100x100 SHS beams. The weight of the loading upper structure was 410 N but the self-weight was not considered in the reported load values. Decks were also instrumented by four displacement transducers measuring vertical deflections at the loading sections and at a distance of 80 mm from the studied support sections (as shown in Figures 11a and 11b).

The failure loads F_u and corresponding displacements at midspan section d_u are summarized in Table 7, where the ultimate reactions R_u (calculated from $R_u = 2/3 \cdot F_u$) are also presented since the resistance of the end supports is investigated. Experimental results reported in [13] for web crushing tests are also reported accounting for the modification for comparison purposes, as for internal support tests, and it can be observed that the obtained ultimate loads were comparable for

both carbon and ferritic stainless steel decks, although slightly higher for ferritics due to strain hardening effects.

Table 7. Experimental results for end support tests on ferritic stainless steel decks (width=1035mm).

Figure 12 presents the load-average deflection curves corresponding to the midspan section for the four end support tests. The deformed shapes of the decks showed considerable deformations at the studied end supports, although overall failure modes involving the loading sections were also observed, as shown in Figures 11c and 11d. As it is appreciated in Figure 12, the influence of the distance from the internal edge of the end support to the end of the deck u is observable but not remarkable, since the reached ultimate loads are almost equal but displacements at collapse are lower for tests with u=60 mm. This might be because the decks with u=60 mm were conducted on previously tested decks (with u=40 mm), being therefore subjected to some initial deformations and residual stresses. Consequently, it can be concluded that previous deck deformation causes a reduction in the deformation capacity, but not in the ultimate load capacity.

Figure 12. Load-displacement curves for end support tests.

3 ASSESSMENT OF EXPERIMENTAL RESULTS FROM SIMPLY SUPPORTED AND CONTINUOUS DECK TESTS

The analysis and assessment of the experimental results obtained from the conducted simply supported and continuous deck tests on ferritic stainless steel decks are presented in this section. Achieved ultimate capacities are compared with those predicted in EN 1993-1-4 [10], which refers to the corresponding clauses in EN 1993-1-3 [11] for carbon steel decking profiles and the applicability of these expressions to ferritic stainless steel decks is evaluated. It should be noted that the effect of the embossments has been neglected in all calculations.

3.1 FLEXURAL CAPACITY OF SIMPLY SUPPORTED DECKS

Since EN 1993-1-4 [10] does not provide supplementary rules for cold-formed members such as decking profiles, provisions given in EN 1993-1-3 [11] for carbon steel need to be considered. According to [11], the bending moment resistance of decks can be estimated from Eq. (1), where

W_{eff} is the effective section modulus, $\sigma_{0.2}$ represents the 0.2% proof stress or the yield stress and γ_{M0} is the partial safety factor for cross-sectional resistance, which has been set to unity in this study to allow the comparison with experimental results. Since the cross-section is non-symmetric about the considered bending axis, two different bending moment resistances (for positive and negative bending) can be calculated. W_{eff} values considering positive and negative bending moment conditions, determined through the Effective Width Method, and the yield strength have already been reported in Table 1 and Table 2, respectively.

$$M_{c,Rd} = \frac{W_{eff}\sigma_{0.2}}{\gamma_{M0}} \quad (1)$$

The comparison of the experimental resistances obtained for simply supported deck tests with the predicted resistances is presented in Table 8. According to these results, EN 1993-1-3 [11] provides quite accurate predictions for the bending moment resistances of ferritic stainless steel decks, although resistances are slightly overestimated when characteristic values of experimental results are considered, which indicates that expressions proposed for carbon steel might be applicable to the tested ferritic stainless steel sheet.

The predicted ultimate moments were calculated by neglecting the embossments but as mentioned before, they can have a significant effect in the final resistance of the decks. Therefore, conclusions should be carefully extracted from the comparison of predicted and experimental loads: the accurate prediction of the moment capacities could indicate that the embossments have no effect in the resistance of the studied stainless steel decks, but could also show that the influence of embossment compensates the influence of different material diagram. This fact is applicable to the bending capacity of the decks as well as for the continuous decks and internal/end support tests. To investigate this, further research should be conducted by testing some additional stainless steel decks without embossments, for example.

Table 8. Experimental and predicted ultimate load values for bending tests.

3.2 FLEXURAL CAPACITY OF CONTINUOUS DECKS

Continuous tests have been used to determine the resistance of the decks that are continuous over two or more spans to combinations of bending moment and concentrated transverse force at internal supports for a given support width. Experimental ultimate loads are compared with the predicted resistances according to EN 1993-1-3 [11] in order to determine whether these proposals are applicable for ferritic stainless steel decking profiles. Besides these comparisons, some additional bending moment evolution analyses are presented.

According to EN 1993-1-3 [11] and EN 1993-1-4 [10], the bending moment-local transverse force interaction at the internal support of the continuous deck determines the ultimate capacity of the system and the required resistance checks are as given in Eqs. (2) to (4):

$$\frac{M_{Ed}}{M_{c,Rd}} \leq 1 \tag{2}$$

$$\frac{F_{Ed}}{R_{w,Rd}} \leq 1 \tag{3}$$

$$R_{w,Rd} = \alpha \cdot n_w \cdot t^2 \sqrt{\sigma_{0.2} E} \left(1 - 0.1\sqrt{r/t}\right) \cdot \left(0.5 + \sqrt{0.02 l_a / t}\right) \cdot (2.4 + (\phi/90)^2)/\gamma_{M1} \tag{4}$$

where F_{Ed} and M_{Ed} are the applied transverse force and bending moment, $R_{w,Rd}$ is the web crippling resistance as in Eq. (4) and $M_{c,Rd}$ is the bending moment resistance of the cross-section, already defined in Eq. (1), and equal to $M_{c,Rk}$=5.8 kNm. The web crippling resistance of the cross-section depends on geometrical parameters such as the internal radius (r), the thickness (t), the number of webs (n_w) and the relative angle between the web and the flange (ϕ). The values of both l_a and α depend on the test configuration and the section type, defined in EN 1993-1-3 [11]. Adopting n_w=10, α=0.15, l_a=60 mm, t=0.8 mm, r=3 mm and ϕ=72°, a web crippling resistance of $R_{w,Rk}$=33.9 kN is obtained from Eq. (4). The interaction between local transverse force and bending moment is considered through Eq. (5), although a modified interaction equation, given in Eq. (6), was suggested by Gozzi [18] after research works on the transverse force-bending moment interaction of austenitic stainless steel cold-formed sections. For the analysed continuous decks, F_{Ed} and M_{Ed} correspond to the reaction and bending moment at the internal support.

$$\frac{F_{Ed}}{R_{w,Rd}} + \frac{M_{Ed}}{M_{c,Rd}} \leq 1.25 \quad \text{interaction expression for carbon steel from EN1993-1-3 [11]} \quad (5)$$

$$\frac{F_{Ed}}{R_{w,Rd}} + \frac{M_{Ed}}{M_{c,Rd}} \leq 1.4 \quad \text{new interaction expression for stainless steel [18]} \quad (6)$$

Since the capacity of continuous decks is governed by the bending moment-local transverse force interaction at the internal support, the analysis of these decks is formulated in terms of the reaction forces at the internal supports. Table 9 presents the experimental reactions corresponding to the middle support collapse $R_{supp,coll}$, measured when the middle support collapse loads $F_{supp,coll}$ reported in Table 4 were recorded. These reactions are compared with the predicted capacities calculated for the interaction expressions presented above. The comparison of the results suggests that the predicted ultimate capacities seem to be conservative for the codified interaction equation given in Eq. (5), and that the revised expression for stainless steel sections Eq. (6) would provide considerably more accurate results. However, it is important to note that the overconservatism observed for the interaction equation codified in EN 1993-1-3 [11] is considerably reduced when the characteristic values of the experimental results are considered as established in EN 1990 [19] or EN 1993-1-3, A6.2 [11], providing accurate resistance predictions.

Table 9. Experimental and predicted ultimate load values for continuous deck tests.

From the measurement of the support reactions and applied loads, the evolution of bending moments at both the internal support and loading sections of the decks is analysed in order to compare these results with the bending moment capacities obtained from the simply supported tests. Predicted bending moments according to linear elastic analysis of the continuous decks are also presented for comparison purposes. Figure 13 presents the evolution of the experimental bending moments at the internal support as the total applied loads increase, compared to the expected linear bending moments. As shown in this figure, the experimental response of the decks differ from the linear elastic behaviour when a total load of about 10 kN is reached, after which a partial moment redistribution is observed and bending moments increase up to the maximum average value of 5.5 kNm. Comparing this value with that obtained from simply supported tests under negative bending moment 5.9 kNm, it can be concluded that the failure of the middle

support section occurs due to bending moment-reaction interaction, which reduces the bending moment capacity of the internal support section.

Figure 13. Experimental and elastic bending moment evolution at internal support.

The bending moment evolution under the loading section closer to the middle support can be also determined from total load and support reaction measurements, and plotted together with the predicted values according to a linear elastic estimation, as shown in Figure 14. The nonlinear behaviour of the deck is evident from this figure, where bending moments start increasing considerably once middle supports fail and moment redistribution occurs.

Figure 14. Experimental and elastic bending moment evolution at loading section.

4 ASSESSMENT OF EXPERIMENTAL RESULTS FOR INTERNAL AND END SUPPORT TESTS

The response of the analysed trapezoidal cross-sections to local transverse forces, including the interaction with bending moment, is analysed in this section for internal and end support tests. From the internal support tests, the moment-rotation diagrams are obtained and the assessment of the available design proposals is presented for ferritic stainless steels, while for end support tests the resistance of the cross-sections is analysed by considering different failure modes.

4.1 INTERNAL SUPPORT TESTS

The resistance of internal supports due to a combined action of bending moment and local transverse force is given by the interaction equations described by Eqs. (5) and (6) already introduced in section 3.2 for continuous decks. The comparison between the experimental and predicted capacities for the conducted internal support tests is presented in Table 10, where the bending moment and web crippling resistances calculated according to EN 1993-1-3 [11] have been considered along with the two interaction expressions given in Eqs. (5) and (6). For the calculation of the predicted ultimate loads F_{pred}, the relationship between the applied load F_{pred}=F_{Ed} and the corresponding bending moment value needs to be considered $M_{Ed} = F_{pred}s/4$. From these results, it seems that both proposals are applicable to ferritic stainless steel decks, and the

interaction equation for stainless steels given in Eq. (6) seems to provide more accurate results. However, readers should keep in mind that a relevant statistical analysis could considerably reduce the conservatism of the interaction expression codified in EN 1993-1-3 [11]. In fact, when the characteristic values of the experimental results are considered, the interaction expression given in EN 1993-1-3 [11] appears to be more accurate for the studied decks. Similar results can be observed from Figure 15, where the experimental results are compared with the interaction equations considered: the continuous line corresponds to the interaction equation given in Eq. (5), while the slashed line represents the revised equation for stainless steels, Eq. (6), and solid markers represent the characteristic values of the obtained experimental results.

Table 10. Experimental and predicted ultimate load values for internal support tests.

Figure 15. Bending moment-local transverse force interaction diagrams and test results.

According to EN 1993-1-3, Annex A [11] *§A.5.2.3*, moment-rotation diagrams should be plotted for each internal support test span. Rotations θ at each load step are derived from experimentally measured deflections from the expression provided in EN 1993-1-3, as given in Eq. (7), where δ_e is the average deflection measured at a distance *e* from the support, δ_{lin} is the fictive net deflection for a given load obtained with a linear behaviour, δ_{pl} is the net deflection for the corresponding load level on the falling part of the curve after F_{max}, *e* is the distance between the deflection measurement section and a support, and *s* is the test span length. The average bending moment-rotation relationships for each test span *s* are plotted in Figure 16.

$$\theta = \frac{2(\delta_{pl} - \delta_e - \delta_{lin})}{0.5s - e} \qquad \text{Eq. (7)}$$

Figure 16. Average bending moment-rotation diagrams of internal support tests for different span lengths.

4.2 END SUPPORT TESTS

The web crushing resistance of cold-formed sections at end supports in EN 1993-1-3 [11] is given by the web crippling equation previously introduced for internal support tests in Eq. (4), but a different category needs to be adopted for the determination of the l_a and α parameters (according

to [11], l_a=10 mm and α=0.075 need to be adopted for end support conditions). The comparison of the predicted capacities with the obtained experimental web crushing resistances is presented in Table 11. It is evident from these results that the predicted resistance is much lower than the ultimate loads achieved during the tests. As mentioned before, EN 1993-1-3 [11] adopts a constant l_a parameter equal to 10 mm for end support tests, while for internal support tests a l_a parameter equal to the load bearing length is defined. Therefore, the same expression for end support conditions but with a different l_a value (equal to the bearing length s_s= 30 mm) has also been considered in Table 11. Nevertheless, results suggest that the EN 1993-1-3 [11] provisions for web crushing are too conservative if the end support test configuration proposed in EN 1993-1-3, Annex A [11] is adopted. It is important to highlight that this test configuration was originally designed for plain decks without embossments and its applicability to cross-sections similar to those used in this study is being revised, since the local transverse resistance of the webs would be probably increased by the embossments.

Table 11. Experimental and predicted ultimate load values for end support tests.

It is important to point out, though, that the failure mechanism on the conducted end support tests was not the typical support section failure under concentrated transverse force. After significant deformation at end supports, decks collapsed due to a bending moment-local force interaction, similar to the internal support tests but not at the end supports. In view of this, end support tests have also been analysed as internal support tests, following the same procedure presented in section 4.1 for a span length of 600 mm and l_a=300 mm. The comparison between the measured ultimate loads F_u and the predicted capacities F_{pred} is presented in Table 12 for the two interaction equations introduced before.

Table 12. Experimental and predicted ultimate load values for end support tests considered as internal supports.

It is evident from this new analysis that the new predicted resistance values are closer to the experimental loads than those shown in Table 11, but are still considerably conservative. In any case, these tests demonstrate that decks will not suffer from early end support collapse and that

the resistance of continuous decks will not be limited by web crushing failure. This suggests that the test setup provided in EN 1993-1-3, Annex A [11] is not adequate for the experimental determination of end support resistances in trapezoidal steel decks and therefore this configuration should be revised. This statement is in line with the conclusions extracted from the RFCS-funded GRISPE project [16], where a new test setup which includes timber blocks in the loading sections is proposed for end support tests in steel decks.

5 CONCLUSIONS

This paper presents a comprehensive experimental study on trapezoidal ferritic stainless steel decks in order to determine the resistance of such structures during construction stage when used as part of composite slabs. The experimental programme comprised several test configurations, which allowed the characterization of the trapezoidal cross-section resistance under different loading conditions. Six tests were conducted on simply supported decks under positive and negative bending conditions, as well as three continuous deck tests over two span structural configurations. In addition, nine internal support tests with different span lengths and four end support tests were carried out. The experimental results showed that expressions codified in EN 1993-1-3 [11] might be, in general, applicable to ferritic stainless steel decks with trapezoidal cross-sections, although some changes may be introduced in order to get more accurate predicting loads. Ultimate loads have also been compared to other experimental results conducted on comparable carbon steel trapezoidal decks under equivalent loading configurations and collapse loads have been found to be similar.

Experimental results on simply supported cold-formed trapezoidal decks showed that the ultimate loads predicted by the existing standards provide safe results for the positive and the negative bending position, indicating that design rules for carbon steel given in EN 1993-1-3 [11] might be applicable to ferritic stainless steels. For continuous decks over two span configurations, the collapse of the continuous decks occurs due to the bending moment-reaction interaction at the internal supports according to [11]. Results suggested that the modified interaction expression proposed by Gozzi [18] for cold-formed stainless steel cross-sections appeared to provide more

accurate results for the studied ferritic decks, although the conservatism observed for the interaction expression codified in [11] is reduced once the characteristic values of the experimental results are considered. This overconservatism is also attributed to the strength reserve obtained from the bending moment redistribution, since the internal support failure occurred at load levels of 90% of the final capacities.

Internal support tests showed similar results regarding the interaction of negative bending moment and local transverse force. The expression in [18] for stainless steel cross-sections was found to provide more accurate results than for the expression given for carbon steel sections in [11], although when characteristic values are considered the expression given in EN 1993-1-3 seems more adequate. Finally, end support tests showed that EN 1993-1-3 [11] provisions for web crushing are too conservative. Nevertheless, it was noticed that the failure mechanism was a bending moment-concentrate load interaction for all the end support tests, failing therefore at the midspan section before the web crushing resistance is reached in outer supports. These tests also highlighted the need of new directions for end support tests in [11] for decks similar to those studied in this paper in order to evaluate the web crushing resistance, which is in line with recent research on steel decks [16].

Once the resistance of trapezoidal ferritic stainless decks in construction stage has been characterized, the study of the performance of such decks as composite slabs needs to be investigated. Complementary tests on long and short composite slabs have been conducted by the authors in order to determine the longitudinal shear resistance according to EN1994-1-1 [9].

ACKNOWLEDGEMENTS

The research leading to these results has received funding from the European Community's Research Fund for Coal and Steel (RFCS) under Grant Agreement No. RFSR-CT-2010-00026, as well as from the Ministerio de Ciencia e Innovación (Spain) under the Project BIA2010-11876-E “Acciones complementarias”.

REFERENCES

[1] Hofmeyer H., Kerstens J.G.M., Snijder H.H. and Bakker M.C.M. Combined web crippling and bending moment failure of first-generation trapezoidal steel sheeting. *Journal of Constructional Steel Research*, 58(12), 1509-1529, 2002.

[2] Mistakidis E. and Dimitriadis K.G. Bending resistance of composite slabs made with thin-walled steel sheeting with indentations or embossments. *Thin-Walled Structures* 46(2), 192-206, 2008.

[3] Lawson R.M. and Popo-Ola S. Load capacity of continuous decking based on small-scale tests. *Thin-Walled Structures*, 69, 79-90, 2013.

[4] Franco J. and Batista E. Buckling behavior and strength of thin-walled stiffened trapezoidal CFS under flexural bending. *Thin-Walled Structures*, 117, 268-281, 2017.

[5] Tan K.H. and Nguyen T.T. Experimental and numerical evaluation of composite floor systems under fire conditions. *Journal of Constructional Steel Research,* 105, 86-96, 2015.

[6] Li G.Q., Zhang N. and Jiang J. Experimental investigation on thermal and mechanical behaviour of composite floors exposed to standard fire. *Fire Safety Journal*, 89, 63-76, 2017.

[7] Baddoo N.R. Stainless steel in construction: A review of research, applications, challenges and opportunities. *Journal of Constructional Steel Research*, 64(11), 1199-1206, 2008.

[8] Cashell K.A. and Baddoo N.R. Ferritic stainless steels in structural applications, *Thin-Walled Structures*, 83, 169–181, 2014.

[9] European Committee for Standardization Eurocode 4. EN 1994-1-1:2004. Design of composite steel and concrete structures. Part 1-1: General rules and rules for buildings. Brussels, Belgium, 2004.

[10] European Committee for Standardization Eurocode 3. EN 1993-1-4:2006+A1:2015. Design of steel structures. Part 1-4: General rules. Supplementary rules for stainless steels. Brussels, Belgium, 2006.

[11] European Committee for Standardization Eurocode 3. EN 1993-1-3:2006. Design of steel structures. Part 1-3: General rules. Supplementary rules for cold-formed members and sheeting. Brussels, Belgium, 2006.

[12] Structural Stainless Steel. Case Study 03: Composite floor at Luxembourg Chamber of Commerce. © 2010 SCI.

[13] Blaβ H.J. and Saal H. Experimentelle Trayfähigkeitsuntersuchung von Stahlblechprofilen COFRADAL 60 PLUS. Fa. PAB Nord Groupe USINOR S.A. Nanterre. Frankreich. 2006. Bericht Nr: 993016-a.

[14] Cofraplus 60. Document Technique d'Application. Référence Avis Technique 3/15-800 (2015). Centre Scientifique et Technique du Bâtiment; http://www.cstb.fr

[15] Arval Plancher Collaborant Cofraplus 60. ArcelorMittal Construction Belgium.

[16] Luure P. and Crisinel M. Essais comparatifs sur tôles nervurees de planchers mixtes avec et sans bossages (Comparison tests for cold-formed sheeting with and without embossments used in composite floors). ICOM-Laboratoire de la Construction Métallique. École Polytechnique Fédérale de Lausanne. Switzerland, 1993.

[17] Pallison A. and Sokol L. WP1 Background guidance for EN1993-1-3 to design of sheeting with embossments and indentations (2013). GRISPE Guidelines and Recommendations for Integrating Specific Profiled steel sheets in the Eurocodes. European Community's Research Fund for Coal and Steel (RFCS) under grant agreement No RFSR-CT-2013-00018.

[18] Gozzi J. Structural Design of Cold Worked Austenitic Stainless Steel. WP3: Cold Formed Profiles and Sheeting Cold Formed Hat and Sheeting profiles - Numerical modelling and design guidance. Final report. Division of Steel Structures, Luleå University of Technology, May 2004.

[19] European Committee for Standardization. EN1990:2005. European Committee for Standardization Eurocode. Basis of structural design. Brussels, Belgium, 2005

FIGURES

Figure 1. Profiled stainless steel decking [12].

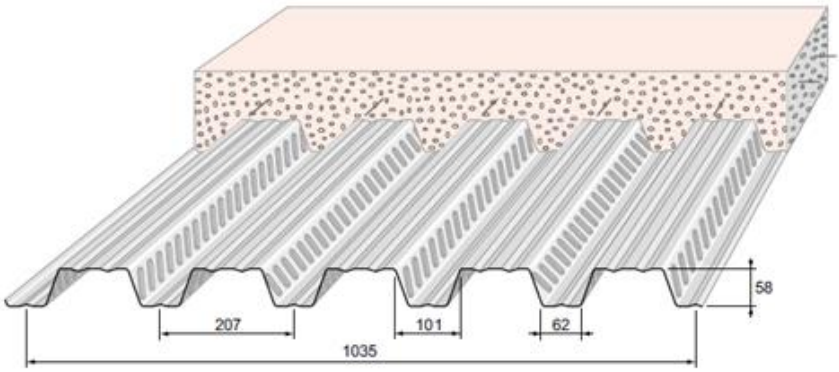

Figure 2. Cofraplus 60 geometry [14].

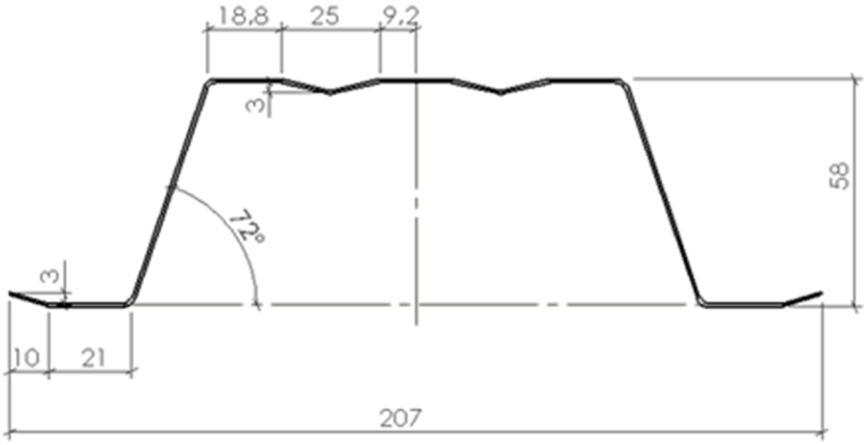

Figure 3. Detailed geometry of a representative wave of the studied deck.

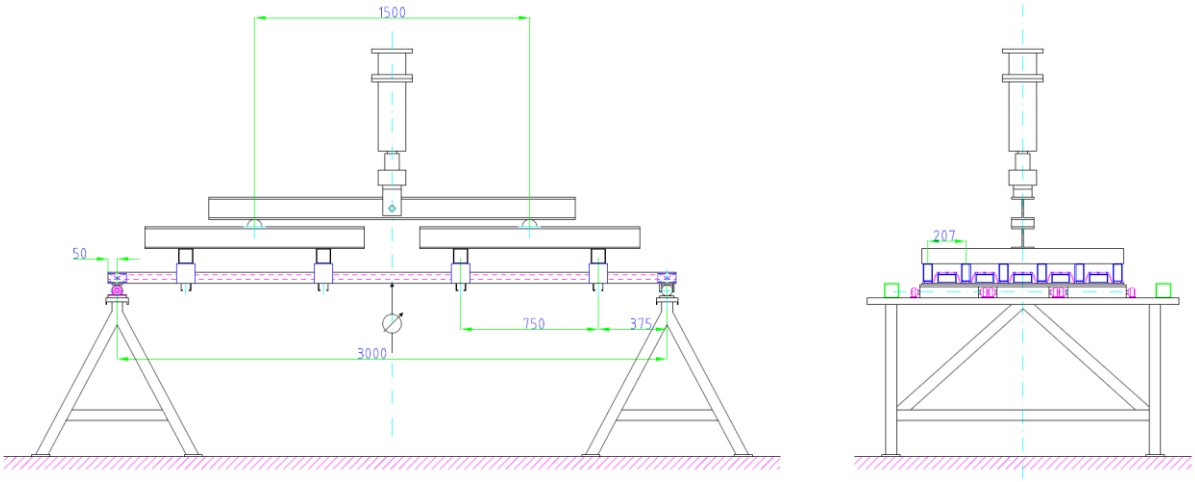

Figure 4a. Test set-up for positive bending M+

Figure 4b. General views of simply supported deck a) test configuration and b) after collapse.

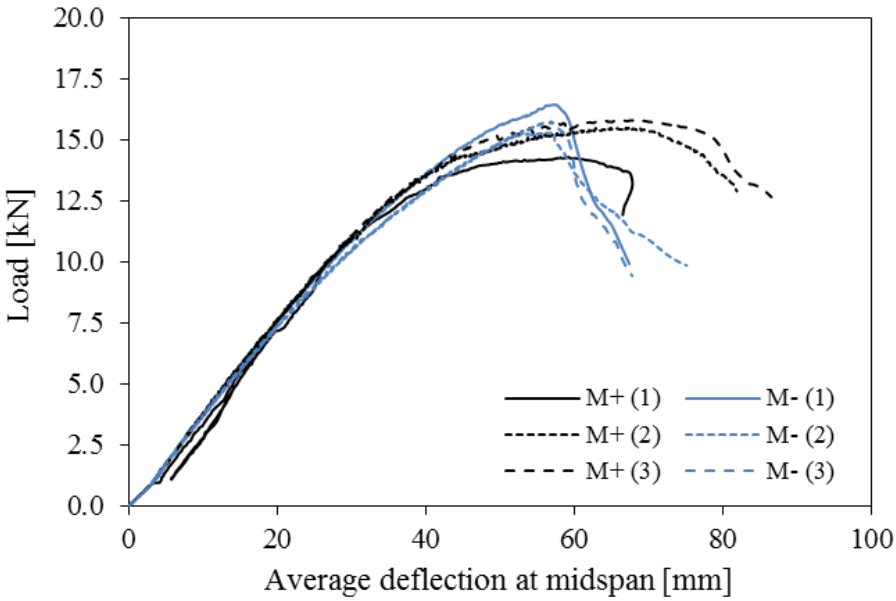

Figure 5. Load-displacement curves for simply supported ferritic stainless steel deck tests.

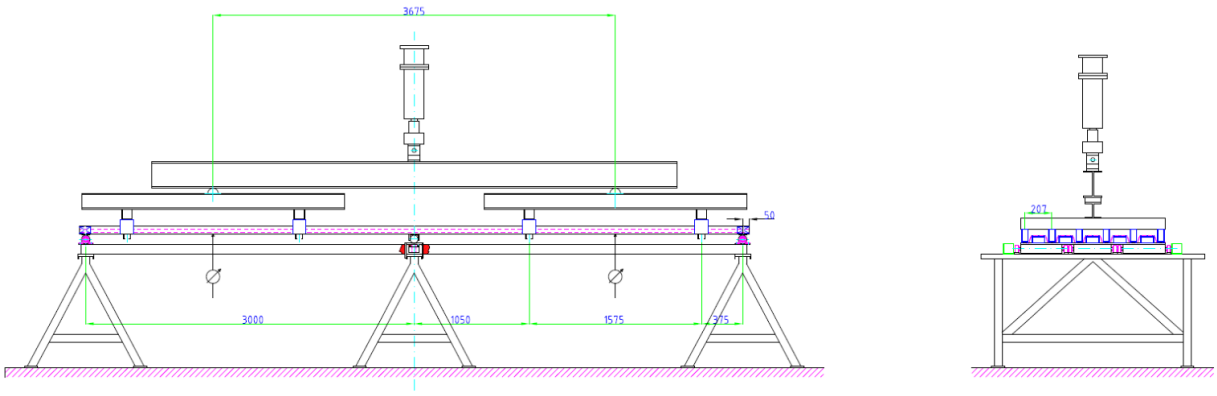

Figure 6. Test set-up for two span bending or continuous deck tests.

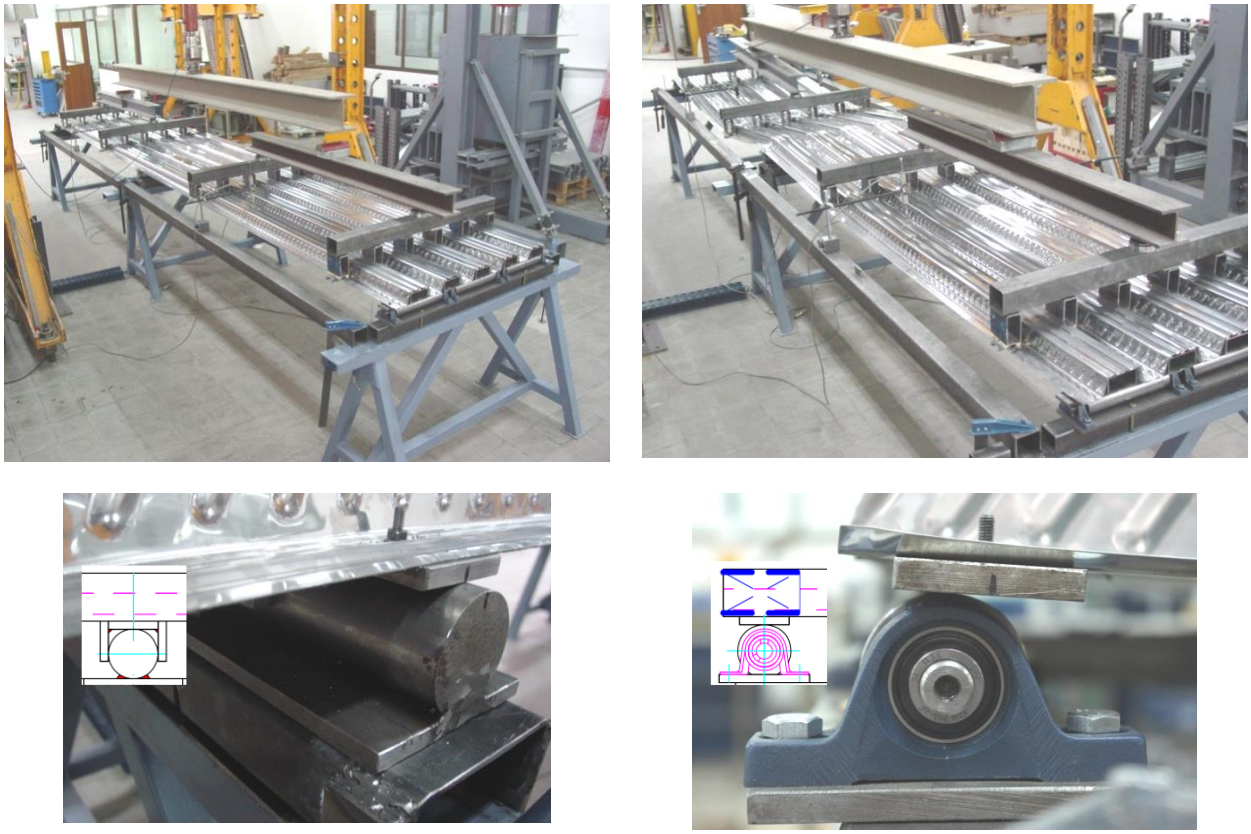

Figure 7. General views of continuous deck a) test configuration and b) after collapse, c) hinged internal support and d) roller external support.

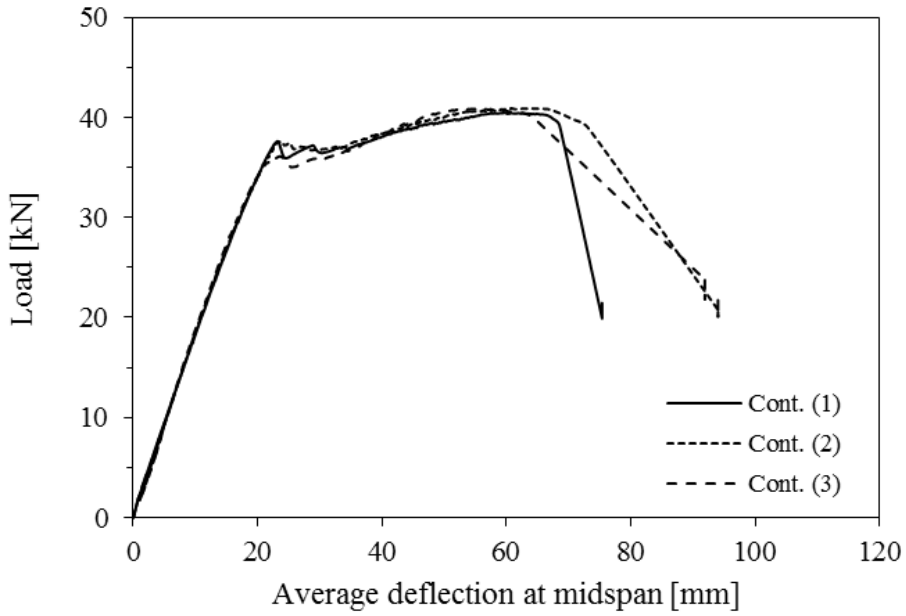

Figure 8. Load-displacement curves for continuous deck tests.


Figure 9. General views of internal support test a) configuration, b) view of the general collapse of the deck, c) lateral view of the general collapse and d) failure of the loading section.

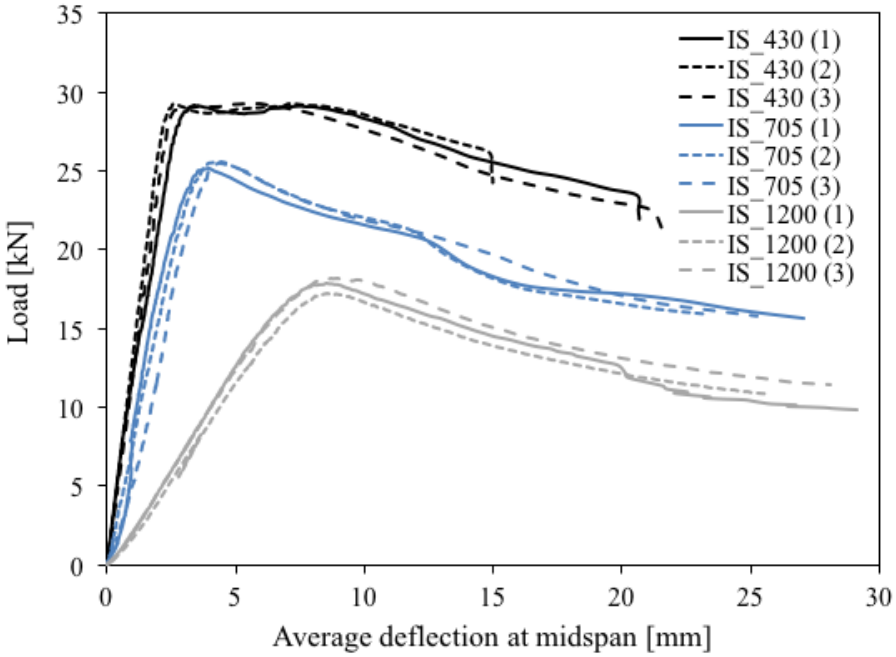

Figure 10. Load-displacement curves for internal support tests.

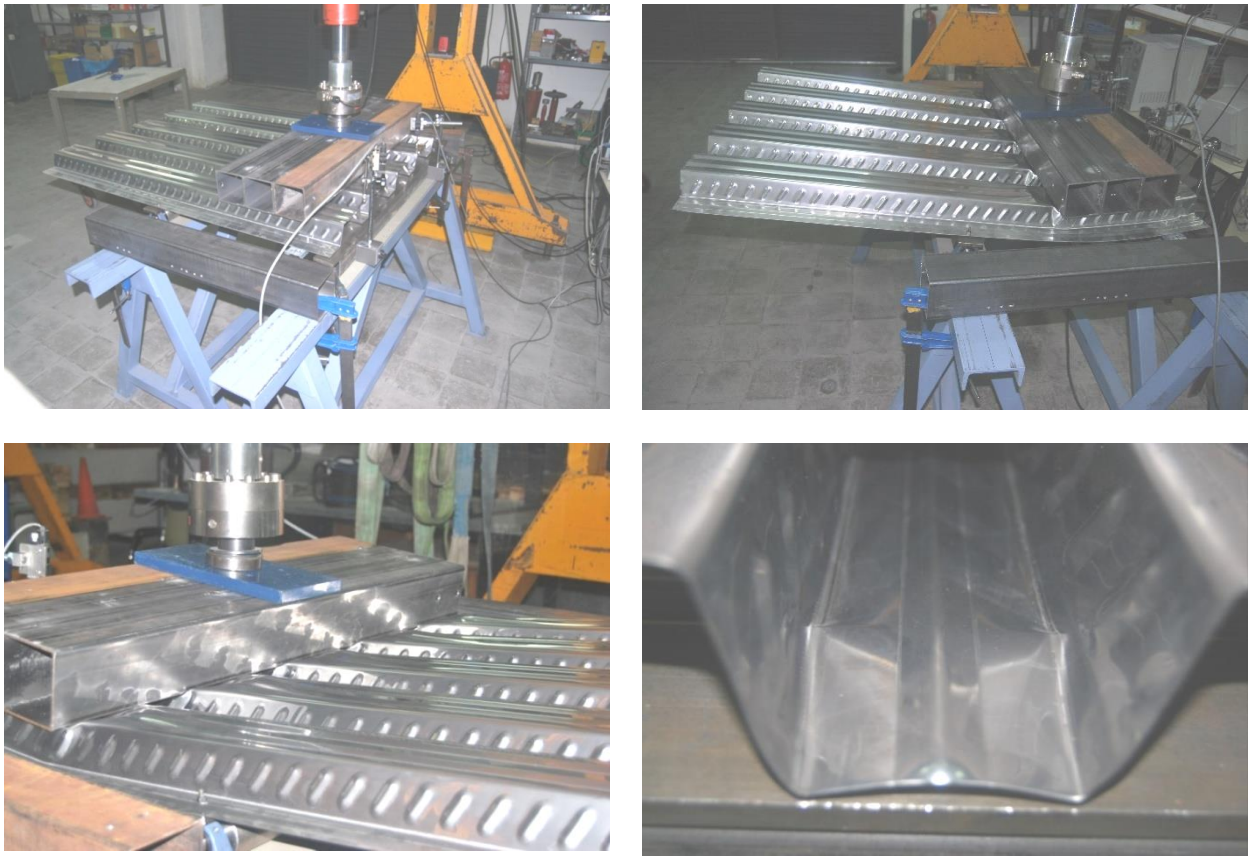

Figure 11. Views of a) end support test configuration for u=40 mm, b) general view of failed deck for u=40 mm, c) detailed view of the collapse of the deck and d) failure of the end support section.

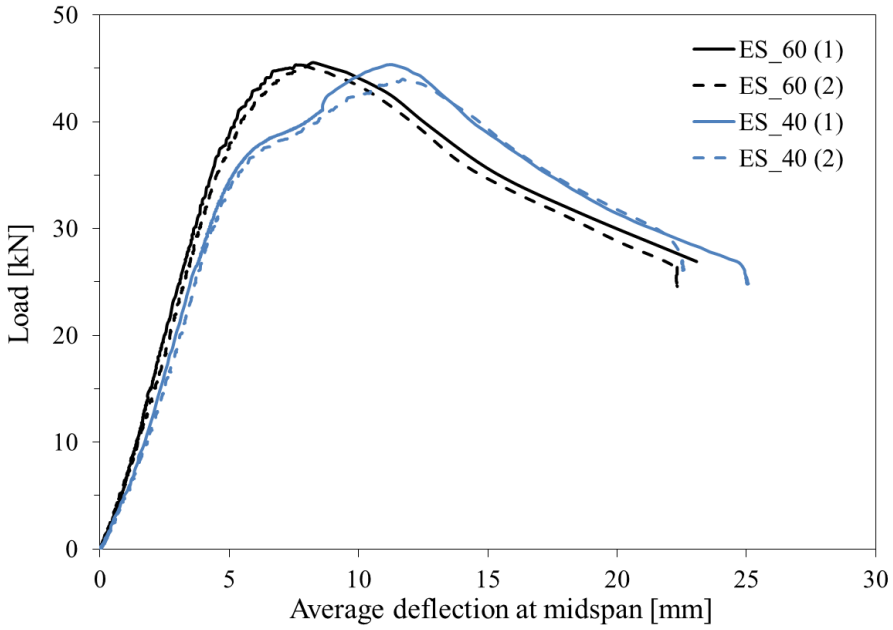

Figure 12. Load-displacement curves for end support tests.

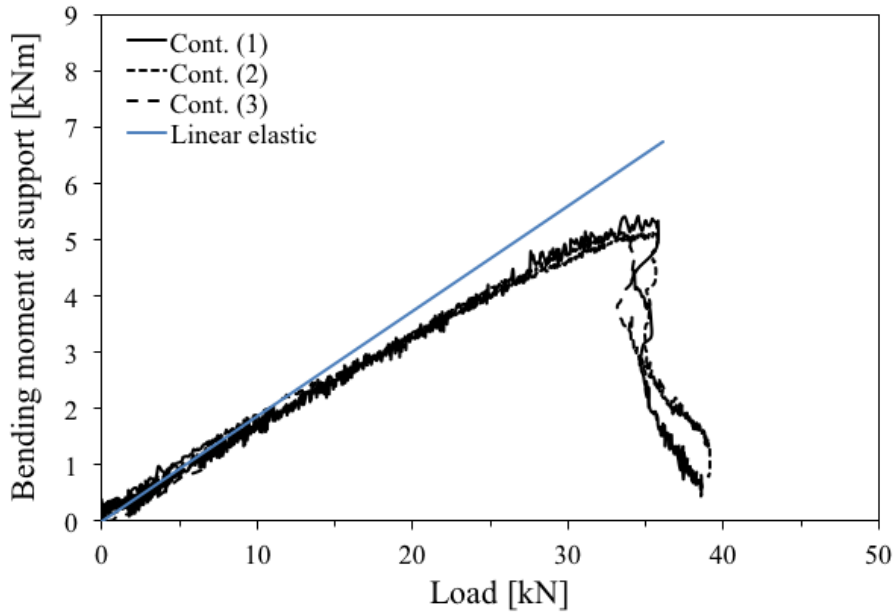

Figure 13. Experimental and elastic bending moment evolution at internal support.

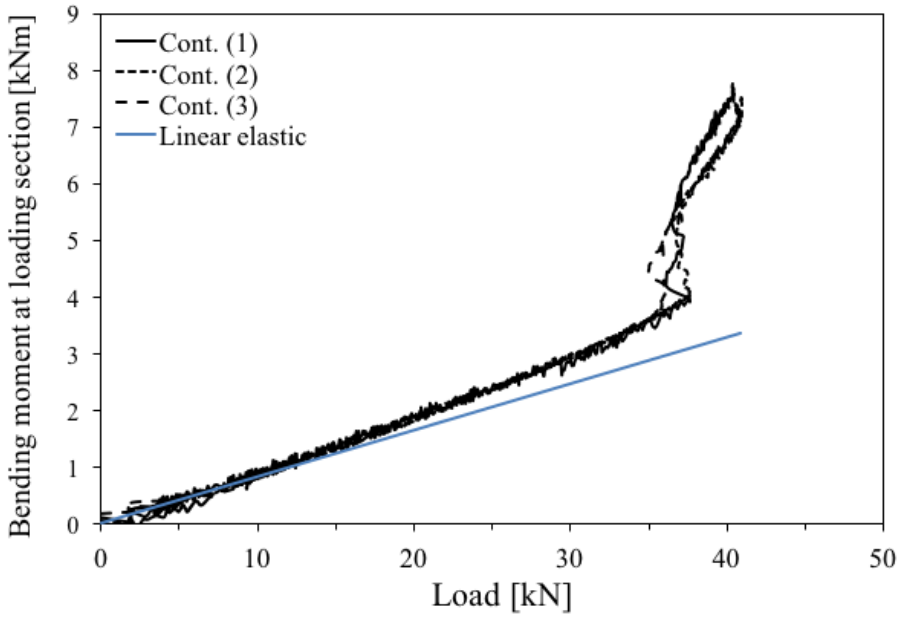

Figure 14. Experimental and elastic bending moment evolution at loading section.

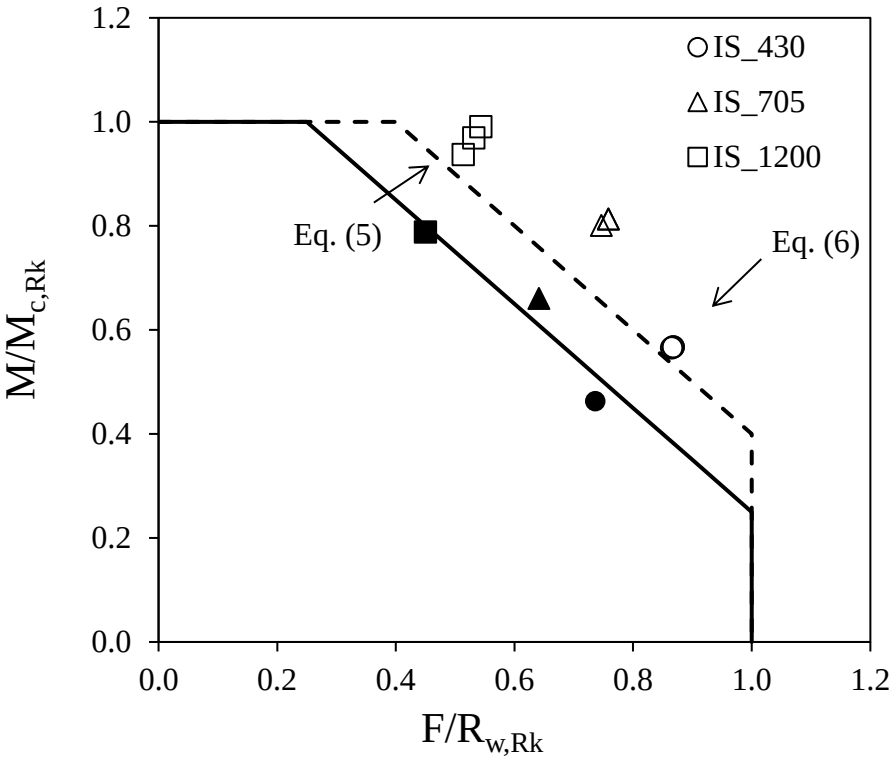

Figure 15. Bending moment-local transverse force interaction diagrams and test results.

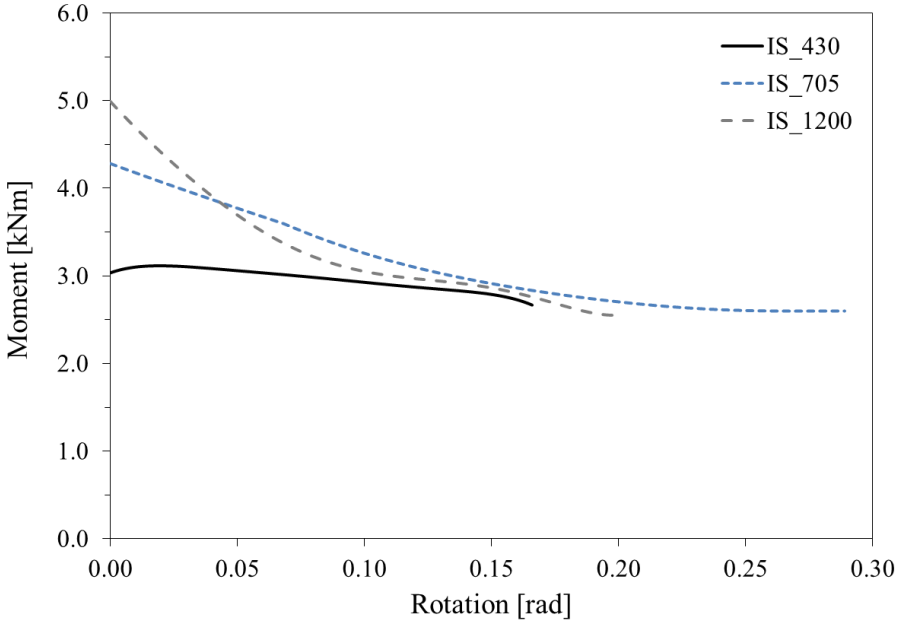

Figure 16. Average bending moment-rotation diagrams of internal support tests for different span lengths.

TABLES

Table 1. Mechanical properties for the studied deck from EN 1993-1-4 [10] and EN 1993-1-3 [11] calculations.

Gross section				Positive bending		Negative bending	
A [cm^2/m]	I_0 [cm^4/m]	W_{el} [cm^3/m]	W_{pl} [cm^3/m]	I_{eff} + [cm^4/m]	W_{eff} + [cm^3/m]	I_{eff} - [cm^4/m]	W_{eff} - [cm^3/m]
11.25	62.26	18.97	23.77	51.98	15.63	60.10	17.78

Table 2. Key material properties of the studied stainless steel deck.

E [MPa]	$\sigma_{0.2}$ [MPa]	σ_u [MPa]	ε_u [%]	*n*	*m*
218 100	326	488	11	12	1.5

Table 3. Summary of key parameter and results from the experimental programme on galvanized steel decks [13].

Material and geometric characterization:		
Measured average yield strength f_y		411 MPa
Measured average tensile strength f_u		490 MPa
Measured average thickness t_m		0.78 mm
Average core thickness t_c		0.78 mm - 0.04 mm = 0.74 mm
Experimental ultimate loads:		
Simply supported, positive bending		14.5 kN
(b_{nom} = 1035 mm, 5 waves)		13.9 kN
		13.9 kN
Simply supported, negative bending		11.1 kN
(b_{nom} = 828 mm, 4 waves)		11.0 kN
		10.3 kN
Internal support tests	s = 430 mm	20.3 kN
(b_{nom} = 828 mm, 4 waves)		20.0 kN
	s = 705 mm	16.7 kN
		16.2 kN
End support tests		43.5 kN
(b_{nom} = 1035 mm, 5 waves)		43.7 kN
		43.1 kN

Table 4. Experimental results for simply supported ferritic stainless steel deck tests (width=1035mm).

		F_u [kN]	M_u [kN·m]	d_u [mm]	M_u from carbon steel tests [13] [kN·m]
Positive bending	M+ (1)	14.3	5.4	56.0	5.4(1)
	M+ (2)	15.5	5.8	65.7	5.1(1)
	M+ (3)	15.8	5.9	64.7	5.1(1)
	Average	15.2	5.7	62.1	5.2(1)
	Charact. value	12.9	4.8	--	4.4(1)
Negative bending	M- (1)	16.4	6.2	54.2	5.1(1,2)
	M- (2)	15.3	5.7	53.2	5.1(1,2)
	M- (3)	15.8	5.9	53.1	4.8(1,2)
	Average	15.8	5.9	53.5	5.0(1,2)
	Charact. value	13.4	5.0	--	4.3(1,2)

(1) After yield strength and thickness corrections for comparison.
(2) After additional correction due to number of waves.

Table 5. Experimental results for continuous ferritic stainless steel deck tests (width=1035mm).

	$F_{supp,coll}$ [kN]	F_u [kN]	d_u [mm]
Cont. (1)	37.2	40.5	59.8
Cont. (2)	37.6	40.9	64.0
Cont. (3)	36.1	40.9	56.0
Average	36.9	40.7	59.9
Charact. value	31.4	34.6	--

Table 6. Experimental results for internal support tests on ferritic stainless steel decks (width=1035mm).

Span length	Test	F_u [kN]	M_u [kN·m]	d_u [mm]	F_u from carbon steel tests [13] [kN]
s = 430 mm	IS_430 (1)	29.3	3.1	3.5	23.7(1,2)
	IS_430 (2)	29.4	3.2	2.7	23.3(1,2)
	IS_430 (3)	29.4	3.2	3.2	--
	Average	29.4	3.2	3.1	23.5(1,2)
	Charact. value	25.0	2.7	--	20.0(1,2)
s = 705 mm	IS_705 (1)	25.3	4.5	4.0	19.5(1,2)
	IS_705 (2)	25.7	4.5	4.3	18.9(1,2)
	IS_705 (3)	25.7	4.5	4.5	--
	Average	25.6	4.5	4.3	19.2(1,2)
	Charact. value	21.8	3.8	--	16.3(1,2)
s = 1200 mm	IS_1200 (1)	18.0	5.4	8.5	--
	IS_1200 (2)	17.4	5.2	8.7	--
	IS_1200 (3)	18.4	5.5	9.0	--
	Average	17.9	5.4	8.7	--
	Charact. value	15.2	4.6	--	--

(1) After yield strength and thickness corrections for comparison.
(2) After additional correction due to number of waves.

Table 7. Experimental results for end support tests on ferritic stainless steel decks (width=1035mm).

		F_u [kN]	R_u [kN]	d_u [mm]	F_u from carbon steel tests [13] [kN]
u = 40 mm	ES_40 (1)	45.8	30.2	11.3	40.5(1)
	ES_40 (2)	44.4	29.3	11.7	40.7(1)
u = 60 mm	ES_60 (1)	45.9	30.3	8.2	40.1(1)
	ES_60 (2)	45.6	30.1	7.9	--
	Average	45.4	30.0	9.8	40.4(1)
	Charact. value	38.6	25.5	--	34.4(1)

(1) After yield strength and thickness corrections for comparison.

Table 8. Experimental and predicted ultimate load values for bending tests.

		Tests	EN1993-1-3 [11]	
		M_u [kNm]	M_{pred} [kNm]	M_{pred}/M_u
Positive bending	M+ (1)	5.4	5.1	0.94
	M+ (2)	5.8		0.88
	M+ (3)	5.9		0.86
	Average	5.7	5.1	0.90
	Charact. value	4.8	5.1	1.06
Negative bending	M- (1)	6.2	5.8	0.93
	M- (2)	5.7		1.02
	M- (3)	5.9		0.98
	Average	5.9	5.8	0.98
	Charact. value	5.0	5.8	1.16

Table 9. Experimental and predicted ultimate load values for continuous tests.

	Experimental $R_{supp,coll}$ [kN]	EN1993-1-3 [11] with Eq. (5) R_{pred} [kN]	EN1993-1-3 [11] with Eq. (6) R_{pred} [kN]
Cont. (1)	17.2	13.5	15.1
Cont. (2)	17.2		
Cont. (3)	16.0		
Average	16.8		
Charact. value	14.3		

Table 10. Experimental and predicted ultimate load values for internal support tests.

Span length		Experimental F_u [kN]	Interaction equation Eq. (5) F_{pred} [kN]	Interaction equation Eq. (6) F_{pred} [kN]
s = 430 mm	IS_430 (1)	29.3	26.0	29.1
	IS_430 (2)	29.4		
	IS_430 (3)	29.4		
	Average	29.4		
	Charact. value	25.0		
s = 705 mm	IS_705 (1)	25.3	20.9	23.4
	IS_705 (2)	25.7		
	IS_705 (3)	25.7		
	Average	25.6		
	Charact. value	21.8		
s = 1200 mm	IS_1200 (1)	18.0	15.4	17.2
	IS_1200 (2)	17.4		
	IS_1200 (3)	18.4		
	Average	17.9		
	Charact. value	15.2		

Table 11. Experimental and predicted ultimate load values for end support tests.

Test	Experimental R_u [kN]	EN1993-1-3 [11] (l_a=10mm) R_{pred} [kN]	EN1993-1-3 [11] (l_a=s_s=30mm) R_{pred} [kN]
ES_40 (1)	30.2	9.8	13.4
ES_40 (2)	29.3		
ES_60 (1)	30.3		
ES_60 (2)	30.1		
Average	30.0		
Charact. value	25.5		

Table 12. Experimental and predicted ultimate load values for end support tests considered as internal supports.

Test	Experimental F_u [kN]	As internal support with Eq. (5) F_{pred} [kN]	As internal support with Eq. (6) F_{pred} [kN]
ES_40 (1)	45.8	31.3	35.1
ES_40 (2)	44.4		
ES_60 (1)	45.9		
ES_60 (2)	45.6		
Average	45.4		
Charact. value	38.6		